

## QUANTITATIVE ANALYSIS OF THERMAL SEA SURFACE STRUCTURES ON NOAA IR-IMAGES

**Alexanin A.I., Alexanina M.G.**

Institute of Automation and Control Processes, Far Eastern Branch, Russian Academy of Sciences,  
Vladivostok, Russia

### Introduction

Infrared (IR) imaging by the NOAA AVHRR, with spatial resolution of approximately 1.1 km, covers the ocean surface several times a day and includes information on synoptic and meso-scale eddy structure. Eddies identification with estimation of their parameters is important task of sea structure analysis. Thermal structures on IR-images are the result of accommodation temperature and sea surface current fields. The forms of thermal structures are explained by shear nature of the sea surface flow, *i.e.* by a variability of the velocity values in the direction perpendicular to the flow. Isotherms are stretched along the flow direction in such current.

Many authors mentioned the accommodation between temperature and velocity fields and some of them attempted to determine velocity characteristics using this property (Essen, 1995; Sugimura *et al.*, 1984; Borisov & Monin, 1989). It is the reason to consider isotherm directions as an approximation of velocity directions. Then identification of synoptic objects may be based on this phenomenon.

Now the problem of identification of eddies and fronts on the sea surface from the satellite images is mainly carried out manually by skilled experts. The identification procedure is based on searching and marking boundaries of the dynamical objects. The procedure takes much time, especially in case of extraction of small-scale features, and it is subjectively depending on the expert knowledge and skill. In addition to this, the manual approach to the identification and analysis of the sea surface dynamics makes difficulties for any computer-aided assimilation of the extraction results.

This work is focused on development of a completely automatic procedure for extraction and parameters estimation of fronts and eddy like objects on sea surface *IR*-images. The procedure is based on a method for calculation of thermal contrast orientations (statistically significant tangents to isotherms in the vicinity of a point).

### Orientation of Radiation Contrasts

The method for marking thermal structures on the sea surface by satellite *IR*-images has been presented (Alexanina, 1997; Alexanin *et al.*, 1998). The marking procedure is based on an approach for extraction of oriented texture from images described by Lemonnier, *et al.* (1994).

Satellite images of the sea surface might be considered as a set of oriented textures in the temperature field, assuming that the field nature is related to the sea dynamics. The oriented structure is a 2D image with a calculated dominant direction of radiation contrast at each point. The method evaluates a dominant orientation of the radiation contrasts and estimates appropriate coherence level (coincidence of the separate orientations) of the local gradient field in the vicinity of every point ( $\nabla u = G_{ij} \cdot \exp(i\varphi_{ij})$ , where  $u$  is the radiate brightness,  $G_{ij}$  is the value of the brightness gradient,  $\varphi_{ij}$  is the angle of the brightness gradient). The angle of radiation contrast direction  $\theta_{ij}$  is determined as the angle of orthogonal direction to the radiation gradient vector.

Determination of the dominant orientation  $\Theta_{mn}$  in the centre  $(m, n)$  of a square of  $N \times N$  size and the coherence  $P$  in its vicinity might be formulated as a minimisation task:

$$\sum \Delta\theta_{ij} \rightarrow \min_{\Theta_{mn}}, \quad (1)$$

$$\text{where, } \Delta\theta_{ij} = W_{ij} \cdot \min\{|\theta_{ij} - \Theta_{mn}|, |\theta_{ij} - \Theta_{mn} - \pi|\}; \quad (2)$$

$W_{ij}$  – a weight coefficient.

The orientation coincidence is based on the Markov's inequality, that allows to estimate probability of an event when a random  $\Delta\theta_{ij}$  exceeds an arbitrary  $\varepsilon$  in absolute value (Alexanina, 1997):

$$P\{\Delta\theta_{ij} < \varepsilon\} > 1 - \frac{M\Delta\theta_{ij}}{\varepsilon}, \quad (3)$$

where,  $M$  – expectation function.

Thus, the structure map of dominant orientations on a satellite IR image is formally determined by setting the permissible variation range  $\varepsilon$  of the dominant orientation and the acceptable probability  $P^*$  of hitting the variation range.

Probability estimation  $P$  is significant by less than one estimated by real outlet of dominants in the vicinity of any point, but it is more convenient in practice because this value allows to determine discrepancy of the thermal contrasts directions.

Previous studies of the algorithm are demonstrated by important properties of dominant orientations. On the sea surface structure map one may see eddies, currents and low contrast structures, which are not clearly visible on the IR image (Fig. 1). Dominant orientations of structure map are highly coincident with velocity directions of flow velocity map (Fig. 2). And again, all information of structure orientations is available in numerals, what is important for a further analysis.

A quantity comparison of dominant orientations and sea surface current directions has been made (Alexanin *et al.*, 2000). Experiments have demonstrated high correlation between dominant orientations and velocity directions of currents (near 0.8). It was shown significant increase in correlation coefficient with velocity values increase (more 0.9, when velocity values were more 30 cm/s). Thus, dominant orientations may be considered as any estimation of current directions.

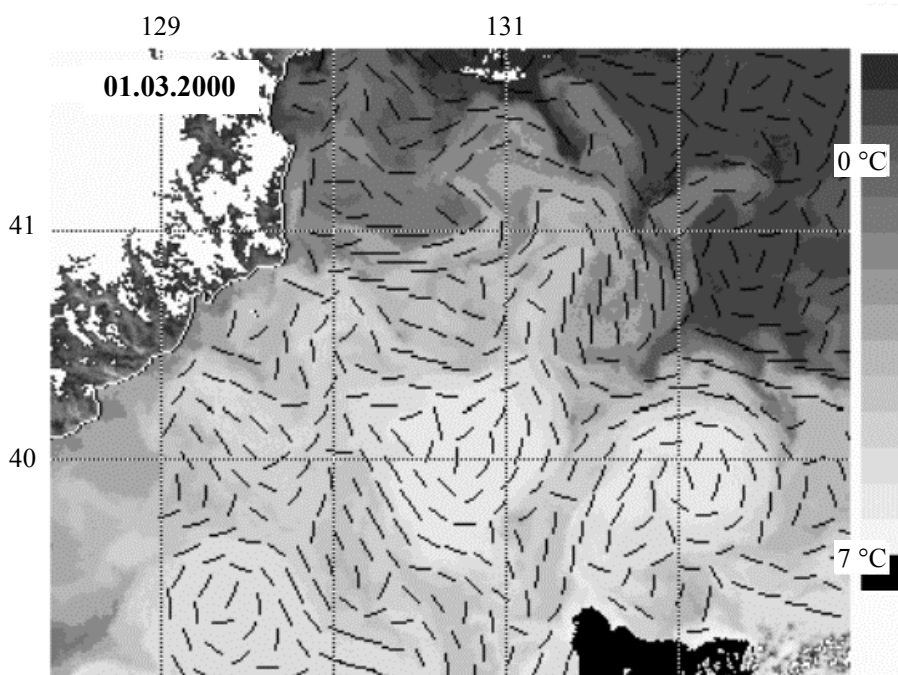


Fig. 1. Single IR-image on 01.03.00 and dominant orientations of thermal contrasts

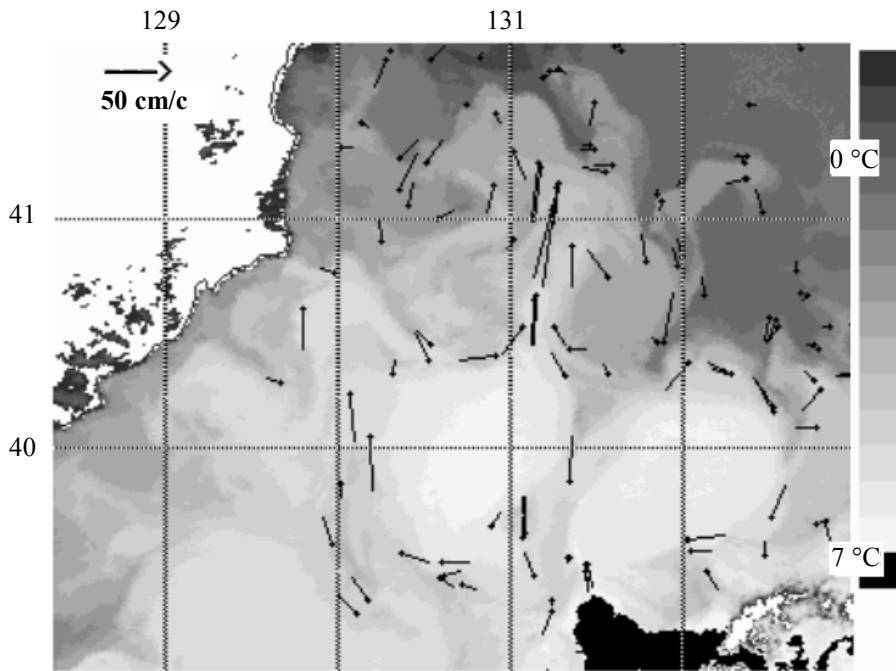


Fig. 2. Sea surface velocities (satellite estimations) and IR-image on 01.03.00

### Eddy Detection Algorithm

High correlation between sea surface velocity directions and dominant orientations of thermal contrasts is explained by shear nature of sea currents. Dominant orientations should be stretched along the current direction in a flow with velocity value decrease from zone of maximum velocity to the flow boundaries. And the more velocity shear, the more close flow direction and thermal contrast orientations (according to the theory of deformation fields (Fedorov, 1987)). A full coincidence should not be. Again, isotherm inclinations on the left and the right sides of a flow should have different sign and incline to the zone of maximum velocity. Thus, according to the theory, inclinations of dominant orientations should detect the flow current direction and location of maximum velocity zone. First version of a method for eddy detection and its parameter determination has been created on the base of these conclusions.

There are two stages of the algorithm. First stage is estimation of eddy locations. Circular model of eddy streamline is used. Velocity directions of a circular motion should be perpendicular to its radius vector, according to the model. It is possible to calculate circular eddy centre on the base of this property, using dominant orientations as velocity directions. Thus, we can calculate a centre of circular moving for any point in its vicinity of radius  $R$ . We can consider this centre as an estimation of eddy location if the discrepancy between the point and calculated centre is less than any small value. We can calculate all eddy location estimations for circular motion of the scale  $R$ , moving along the chart of dominant orientations.

Second stage of algorithm is calculation of eddy parameters of shape and location on the base of elliptic model of motion, using the points of the first stage as initial approximations of eddy locations.

#### Stage 1. Detection of an Eddy Centre Location

Calculation of eddy centre coordinates  $X_0=(x_0,y_0)$  for a point  $X_l=(x_l,y_l)$  in its vicinity of radius  $R$ :

$$\min_{x,y} 1/N \cdot \sum_i W_i(r'_i, d_i)^2, \quad (3)$$

$$\text{where, } i - \|X_i - X_0\| \leq R, \quad X_i = (x_i, y_i); \quad (4)$$

$$r'_i = (x_i - x, y_i - y); \quad (5)$$

$$\text{orientation } d_i = (\cos \Theta_i, \sin \Theta_i); \quad (6)$$

$$(r'_i, d_i) - \text{scalar product,}$$

$W_i$  – weight coefficient.

From the optimality conditions for (3):

$$x_0 = (\gamma S_2 - \beta S_1) / (\gamma^2 - \xi \beta), \quad y_0 = (\xi S_2 - \gamma S_1) / (\gamma^2 - \xi \beta), \quad (7)$$

$$\xi = \sum W_i \sin^2 \Theta_i, \quad (8)$$

$$\gamma = \sum W_i \sin \Theta_i \cos \Theta_i, \quad (9)$$

$$\beta = \sum W_i \cos^2 \Theta_i, \quad (10)$$

$$S_1 = \sum (x_i W_i \sin^2 \Theta_i - y_i W_i \sin \Theta_i \cos \Theta_i), \quad (11)$$

$$S_2 = \sum (x_i W_i \sin \Theta_i \cos \Theta_i - y_i W_i \sin^2 \Theta_i). \quad (12)$$

Detection criteria:  $\|X_1 - X_0\| < \delta$ .

Quality criteria – discrepancy between dominants and velocity directions of the circular model:

$$f_o = \sum W_i (\Delta \Theta_i - \pi / 4) < 0, \quad (13)$$

$$\text{where, } \Delta \Theta_i = \left| \arccos \left\{ \left[ -\sin \Theta_i (x_i - x_0) + \cos \Theta_i (y_i - y_0) \right] / \|r_i\| \right\} \right|. \quad (14)$$

### Stage 2. Eddy Parameter Calculation

Elliptic model:

Radial distance:

$$r = \left\{ \left[ (x - x_0) \cos \alpha + (y - y_0) \sin \alpha \right]^2 + \left[ -(x - x_0) \sin \alpha + (y - y_0) \cos \alpha \right]^2 \right\}^{0.5}, \quad (15)$$

$$0 \leq r \leq R$$

Eddy parameters

$$G^* = \{x_0, y_0, R, \varepsilon, \alpha\}, \quad (16)$$

where,  $(x_0, y_0)$  – eddy center;

$R$  – scale;

$\varepsilon$  – eccentricity;

$\alpha$  – angle of ellipse large axis.

Parameters calculation:

$$\min f_o + f_s, \quad (17)$$

$$\text{where, } f_o = \sum W_i (\Delta \Theta_i^* - \pi / 4); \quad (18)$$

$$0 < \|r_i\| < R; \quad (19)$$

$$f_s = \max \left[ 0, \sum W_i (\pi / 4 - \Delta \Theta_i) \right] R < \|r_i\| < 1.5R; \quad (20)$$

$\Delta \Theta_i^*$  – angle of tangent direction of flow line in a point  $(x_i, y_i)$ ;

$$\Delta \Theta_i^* = \min \left( \left| \Theta_i^* - \Theta_i \right|, \left| \pi - \Theta_i^* + \Theta_i \right| \right), \Theta_i^*. \quad (21)$$

In (17)  $f_o$  – quality criteria for elliptic model,

$f_s$  – penalty function (for correct calculation of eddy boundaries).

Maximum velocity zone location ( $r_{max}$ ):

$$MaxS_L - S_R, S_L = \sum_r S_i, 0 \leq r_i \leq r, \quad (22)$$

$$S_R = \sum s_i, r \leq r_i \leq R, \quad (23)$$

where,  $s_i = sign(r_i, d_i)$  – the sign of scalar product.

### Time Averaging of Dominant Orientation Field

It is useful to calculate time averaged dominant orientation field for one-two day time interval before using the eddy detection algorithm. It was shown (Alexanin *et al.*, 1999) that significant amount of dominants loses time stability during first 12 hours. And dominant orientation demonstrates time stability, then it is a contrast orientation of meso-scale object (eddy, front).

It was used follow time averaging scheme. Time averaging dominant orientation  $\Theta_c$ :  $\Theta_c = (\sum \Theta_i \cdot P_i) / (\sum P_i)$ , where  $\Theta_i$  and  $P_i$  are the angle of dominant orientation and appropriate statistical significance on a time moment  $i$ ,  $N$  – amount of images. Statistical significance of time dominant orientation  $P_c$ :

$$P_c = M(P_i) \cdot P_M, \quad (24)$$

where  $M(P) = (\sum P_i) / N$ , (25)

$$P_M = P\{|\Theta_i - \Theta_c| < \varepsilon\}. \quad (26)$$

### Eddies Detection

It was made an experiment for the algorithm testing. The purpose was to detect eddies with radius near 30 km. Detection criteria  $\delta$  was taken 4 km. It was used a satellite IR-images on 01-02.03.2000. Algorithm presented was used to detect eddies and to calculate its parameters  $G_i$  by averaged dominant orientations field presented in Fig. 3. Black rhombuses are results of the first stage of the algorithm. Its sizes are proportion to the quality criteria values (the more, the better). Ellipses are the boundaries of main eddies for a region selected (white rectangle), which have been calculated at the stage 2 of the algorithm. There are the IR-image and sea surface velocity vectors for comparison in Fig. 2.

The algorithm calculated 8 groups of points. Point locations are usually near the centres of water circulation motions and have not significant contradiction with flow velocity field. The shapes and locations of three main eddies are appropriate to the reality (eddies monitoring was carried out during two months).

#### Shear Nature of the Sea Surface Flow Field

The shear character of sea surface flow field explains the good correlation of current velocity vectors with radiation contrast orientations. An experiment was carried out for more complete demonstration of this statement and quantitative estimation of the method calculations.

Current velocities were derived by satellite images (manual feature tracing method, Fig. 4) for an anticyclone eddy in the Okhotsk Sea. Geometrical parameters of the eddy were evaluated on the base of eddy elliptic model (15).

Parameters evaluation procedure for  $G^*$ :  $\min \sum \|V_n^i\|$ , where  $V_n^i$  – normal velocity component (Fig. 4b).

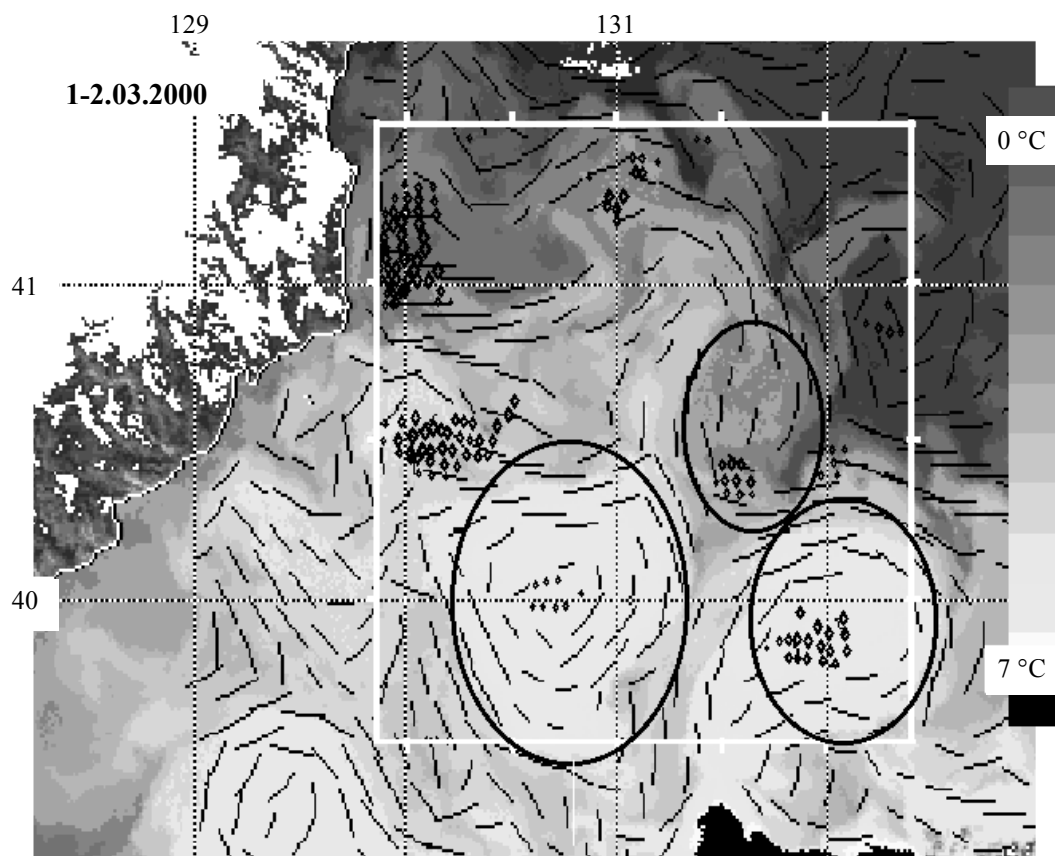


Fig. 3. Time averaged dominant orientations on 1-2.03.2000, points, which can be used as a first estimation of eddy centre locations (black rhombuses), and boundaries calculated for the main eddies (elliptic curves)

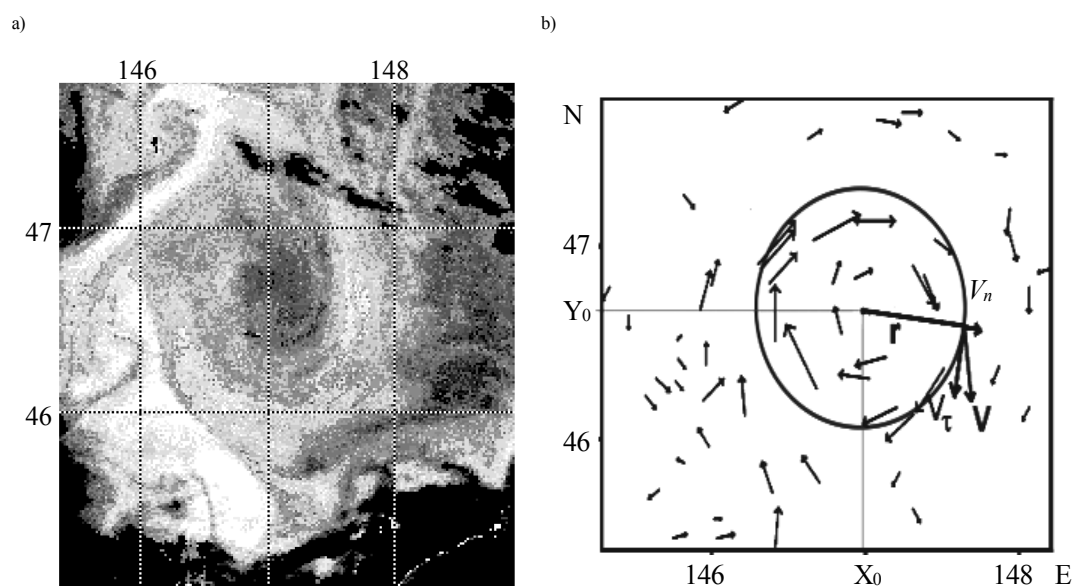


Fig. 4. a) IR-image of an eddy in the Okhotsk Sea.  
b) Sea surface velocity vectors (satellite estimations) and streamline of elliptic model of the eddy with the centre  $(X_0, Y_0)$ .  $V_n$  and  $V_t$  – normal and tangent components of a velocity vector  $V$

Calculation of optimum parameters was carried out by methods of non-linear programming. As a result, the eddy model is almost circular. The purpose of experiment was to compare radial profiles of current velocities and dominant orientations. It was calculated tangential (perpendicular to radius) and normal (along radius) components of the velocity and dominant orientation vectors and its locations along

the eddy radius.

Results are presented in Fig. 5. Tangential components of sea surface flow velocities ( $V_t^i$ ) are in the right diagram. Brightly expressed zone of the maximal velocities may be seen in the diagram. Dominant orientations averaged by 10 kilometre intervals and proportional to their statistical significance are submitted in the left diagram.

The shear character of sea surface flow field is well demonstrated in the given diagrams, that is:

- dominant orientations have a slope to the zone of maximal velocities (as expected);
- velocity value shear on the left side is stronger than on the right and therefore dominant orientations on the left have a smaller rejection from current direction;
- there is a decrease in the dominant orientation statistical significance to the eddy periphery.

It was estimated the eddy parameters by dominant orientation field for quantitative evaluation of results of eddy detection algorithm work. It was used the same calculation scheme. The results were almost the same. Location discrepancy was near 4 km. Other eddy parameters have difference less 10%, only the length of small axis had discrepancy near 20%. The appreciation of maximum velocity zone was satisfactory.

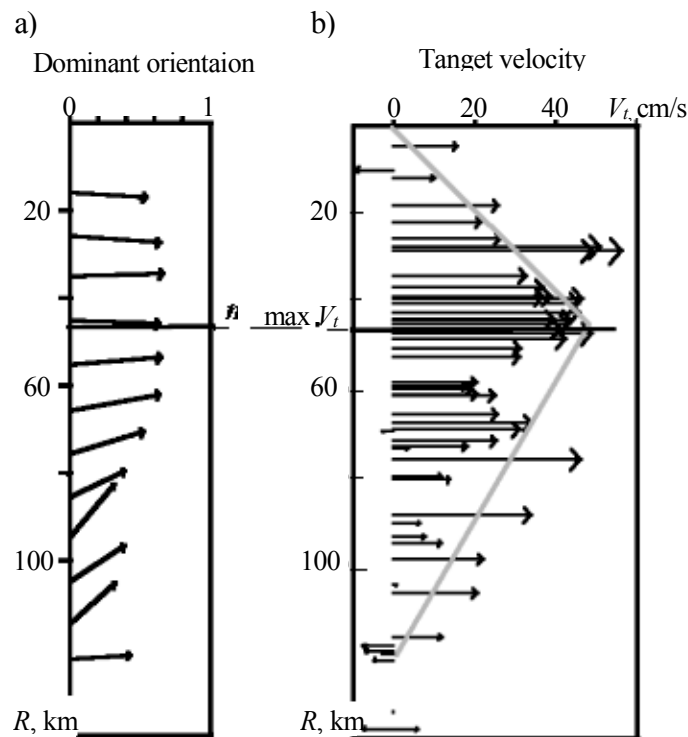


Fig. 5. Eddy radial profiles of: a) dominant orientations of thermal contrasts and b) tangent velocity components ( $V_t^i$ ). The figure demonstrates inclination of thermal contrast orientations to the zone of maximum velocity values. The lengths of thermal contrast orientations are proportional to its statistical significance

## Conclusions

A new approach for automatic detection of eddies and its parameter appreciation on satellite IR-images of a sea is considered. A preliminary processing of images is used for calculation of dominant orientations of thermal contrasts. The processing is based on a method for oriented texture analysis, presented some years ago. Statistically significant thermal contrast directions have high correlation with sea surface velocity directions and are considered as its estimation. Such dominant orientation behaviour is explained by the shear property of a sea velocity field and it may be used for eddy detection and its parameter calculation.

A variant of eddy detection method is presented and tested. The method is used for appreciation of eddy centre location, its shear and location of maximum velocity zone. First results have demonstrated that approach proposed is rather promising for detection and quantitative monitoring of eddies and fronts.

This work was partly supported by Russian Foundation for Basic Research (Grants N 97-01-00107 and N99-01-00639).

### References

1. Alexanin A.I., Alexanina M.G. & Gorin I.I. 2000. Satellite infrared images: from thermal structures to velocity field / *Earth Research from Space* (in press).
2. Alexanin A.I., Alexanina M.G. & Gorin I.I. 1999. Thermal sea surface structures on NOAA IR-imagery: time-scaling variability and association with sea surface flows // *PICES-VIII Annual Meeting*. Vladivostok. Russia P. 77.
3. Alexanin A.I., Alexanina M.G., Herbeck E.E. & Ryabov O. 1998. Scaling property estimation of thermal sea surface turbulent structures on NOAA IR-imagery // *Proc. OCEANS'98*. Nice. Vol. 2. P. 1000-1005.
4. Alexanina M.G. 1997. Automatic detection oceanic surface structures from infrared data of NOAA satellites // *Earth Research from Space*. N 3. P. 44-51.
5. Borisov S.B., Monin A.S. 1989. About temperature and current correlation in the Ocean // *Trans. USSR Academy of Science*. Vol. 306. N 5. P. 1230-1233.
6. Essen H.H. 1995. Geostrophic surface current as derived from satellite SST images and measured by a land-based HF radar // *J. Remote Sensing*. Vol. 16. N 2. P. 239-256.
7. Fedorov K.N. 1987. Physical nature and structure of ocean fronts / Leningrad: Gidrometeoizdat. 512 pp.
8. Lemonnier B., Delmas R., Lopez C. & Duporte E. 1994. Multiscale analysis of shapes applied to thermal infrared sea images // *Proc. Ocean'94 OSATES*. Brest. Vol. 3. P. 319-322.
9. Mullen G.P. 1996. Modeling of the meandering Gulf Stream using satellite imagery and surface drifter data: *Abstr. 21<sup>th</sup> Gen. Assem. Eur. Geophys. Soc., Hague* // *Ann. geophys.* Vol. 14. Suppl. N 1. P. 57.
10. Sugimura T., Tanaka S. & Hatakeyama Y. 1984. Surface temperature and current vectors in the Sea of Japan from NOAA-7 AAVHRR data // *Remote sensing shelf sea hydrodyn. Proc. 15 Int. Liege. Colloq. Amsterdam*. P. 133-147.